

Phase Unwrapping in Correlated Noise for FMCW LIDAR Depth Estimation

Ulvog, Alfred; Rapp, Joshua; Koike-Akino, Toshiaki; Mansour, Hassan; Boufounos, Petros T.;
Parsons, Kieran

TR2023-028 May 06, 2023

Abstract

In frequency-modulated continuous-wave (FMCW) lidar, the distance to an illuminated target is proportional to the beat frequency of the interference signal. Laser phase noise often limits the range accuracy of FMCW lidar, and existing frequency estimation methods make overly simplistic assumptions about the noise model. In this work, we propose an algorithm that performs frequency estimation via phase unwrapping by explicitly accounting for correlations in the phase noise. Given a candidate frequency, we approximately recover the maximum likelihood unwrapping sequence using the Viterbi algorithm and the phase noise statistics. The algorithm then alternates between unwrapping and frequency estimate refinement until convergence. Compared to state-of-the-art alternatives, our algorithm consistently achieves superior performance at long range or with large-linewidth lasers when the signal-to-noise ratio is sufficiently high.

*IEEE International Conference on Acoustics, Speech, and Signal Processing (ICASSP)
2023*

PHASE UNWRAPPING IN CORRELATED NOISE FOR FMCW LIDAR DEPTH ESTIMATION

A. Ulvog*, J. Rapp, T. Koike-Akino, H. Mansour, P. Boufounos, K. Parsons

Mitsubishi Electric Research Laboratories (MERL), Cambridge, MA 02139, USA

ABSTRACT

In frequency-modulated continuous-wave (FMCW) lidar, the distance to an illuminated target is proportional to the beat frequency of the interference signal. Laser phase noise often limits the range accuracy of FMCW lidar, and existing frequency estimation methods make overly simplistic assumptions about the noise model. In this work, we propose an algorithm that performs frequency estimation via phase unwrapping by explicitly accounting for correlations in the phase noise. Given a candidate frequency, we approximately recover the maximum likelihood unwrapping sequence using the Viterbi algorithm and the phase noise statistics. The algorithm then alternates between unwrapping and frequency estimate refinement until convergence. Compared to state-of-the-art alternatives, our algorithm consistently achieves superior performance at long range or with large-linewidth lasers when the signal-to-noise ratio is sufficiently high.

Index Terms— Frequency-modulated continuous-wave lidar, phase unwrapping, generalized least squares, Viterbi algorithm

1. INTRODUCTION

Lidar is an increasingly popular sensing modality for ranging applications varying from autonomous driving to industrial robotics. Frequency-modulated continuous-wave (FMCW) lidar is particularly attractive because it is less sensitive than conventional pulsed lidar to ambient light or interference from other sensors [1]. Like the related technique of swept-source optical coherence tomography (SS-OCT), FMCW lidar is a coherent ranging technology that measures distance by mixing a local copy of the transmitted laser beam with the light reflected back to the receiver. The beat frequency of the resulting interference signal is proportional to the reflector range, so distance measurement becomes a frequency estimation problem.

The limiting factor for FMCW accuracy is often considered to be the laser source phase noise. As illustrated in Fig. 1, laser phase noise causes the interference signal to deviate from the true beat frequency. For a laser whose *frequency noise* (the first derivative of the phase noise) is white and Gaussian, the resulting interference signal has a power spectral density (PSD) that asymptotically approaches a Lorentz distribution as the range increases [2]. On the contrary, classical frequency estimation settings assume a pure sinusoid in *additive* white Gaussian noise (AWGN), for which the maximum likelihood estimate is the peak of the periodogram [3]. However, peak-finding methods perform poorly when the signal power is distributed over a range of frequencies. Kim et al. show improved performance at long distance by fitting a Lorentzian function to the signal spectrum PSD [4], but the Lorentzian fitting has limited precision at high signal-to-noise ratio (SNR).

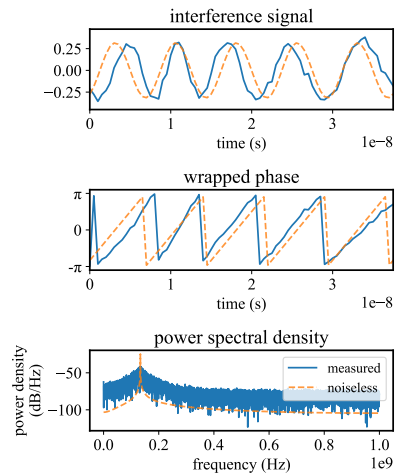


Fig. 1: In an FMCW lidar interference signal, laser phase noise causes variation in the beat frequency, decreasing the periodicity of the phase and broadening the signal’s power spectral density.

Instead, we estimate the frequency in the time domain by performing phase unwrapping followed by linear regression. However, existing phase unwrapping methods do not take phase noise into account, which can lead to errors in the regression stage [5, 6, 7, 8, 9]. Inspired by the fast least squares phase unwrapping estimator (FLSPUE) [8], we propose an algorithm for frequency estimation via phase unwrapping that takes advantage of correlated phase error. We propose an unwrapping approach that uses an initial frequency estimate to predict the phase error via the linear minimum mean squared error (LMMSE) estimator and then approximately recovers the most likely unwrapping sequence via the Viterbi algorithm [10]. After unwrapping, the frequency estimate is refined via generalized least squares (GLS) regression. By both applying the known phase noise statistics and alternating between phase unwrapping and frequency estimation, our iterative algorithm empirically converges better than other methods, enabling the use of as little as one initial frequency, and outperforming the state-of-the-art Lorentzian fitting at sufficiently high SNR.

2. FMCW LIDAR MODEL

2.1. Optical Signal Model

Here we summarize the basic FMCW lidar modeling from Vasilyev [11, Ch. 2], with definitions illustrated in Fig. 2. An FMCW lidar measurement is made by linearly sweeping the frequency of a tunable laser and splitting the swept beam into two channels: a lo-

*A. Ulvog is a PhD student at Boston University, Boston, MA, USA. This work was performed during an internship at MERL.

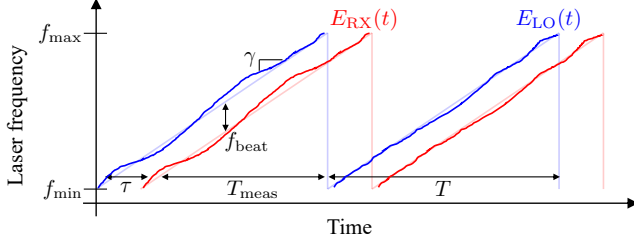


Fig. 2: FMCW lidar definitions. Laser phase noise causes the instantaneous frequency to deviate from the expected linear modulation.

cal oscillator (LO) and a transmitter (TX). Transmitted light that is reflected from a target is captured by the receiver (RX) and optically mixed with the local oscillator. Let T be the sweep duration, ϕ_0 the initial phase, ω_0 the initial angular frequency, γ the chirp rate, and ϕ_n the source phase noise. Within one chirp period, the LO channel has normalized electric field

$$E_{LO}(t) = \text{rect}\left(\frac{t - T/2}{T}\right) \cos\left(\phi_0 + \omega_0 t + \frac{\gamma t^2}{2} + \phi_n(t)\right). \quad (1)$$

The received signal electric field $E_{RX}(t) = \sqrt{R}E_{LO}(t - \tau)$ has been scaled by the target reflectivity R and delayed by $\tau = 2d/c$, where d is the target distance and c is the speed of light. The LO and RX fields are summed at the coherent receiver, and the low-pass filtered intensity is measured by a detector, with measurement window T_{meas} ensuring overlap of the mixed chirps.

FMCW receivers often use a single balanced detector to capture the *in-phase* interference measurement

$$i_I(t) = \sqrt{R} \cos\left[\omega_0 \tau - \frac{\gamma \tau^2}{2} + \gamma \tau t + \Delta\phi_n(t; \tau)\right] + w_I(t), \quad (2)$$

where $\Delta\phi_n(t; \tau) = \phi_n(t) - \phi_n(t - \tau)$ is the phase change¹ and w_I is approximately additive white Gaussian noise (AWGN) with variance $\sigma_w^2/2$. For phase extraction, the *quadrature* component could be approximated by $\hat{i}_Q(t) = \mathcal{H}\{i_I(t)\}$, but the Hilbert transform $\mathcal{H}\{\cdot\}$ introduces errors in the phase. To more accurately extract the phase of the interference signal, we assume the use of a 90° optical hybrid with two pairs of balanced detectors [13], which also records the quadrature measurement

$$i_Q(t) = \sqrt{R} \sin\left[\omega_0 \tau - \frac{\gamma \tau^2}{2} + \gamma \tau t + \Delta\phi_n(t; \tau)\right] + w_Q(t), \quad (3)$$

where w_Q and w_I are independent and identically distributed. The phase is extracted as $\text{atan2}(i_Q(t), i_I(t))$.

2.2. Sampled Signal Model

To simplify notation, we rewrite the observed signal as a complex-valued sinusoid

$$\begin{aligned} r(t) &= i_I(t) + j i_Q(t) \\ &= a \exp\{j2\pi[ft + \theta + \eta(t)]\} + w(t), \end{aligned} \quad (4)$$

where $a = \sqrt{R}$ is the signal amplitude, $f = \gamma\tau$ is the beat frequency, $\theta = \omega_0\tau - \gamma\tau^2/2$ is the phase offset, $\eta(t) = \Delta\phi_n(t; \tau)$ is

¹Since *phase noise* refers to variation in the phase of an oscillator such as a laser, we follow [12, Ch. 7.6.1] in using the term *phase change* to describe the resulting phase error in an interferometric measurement.

a stationary random process denoting the phase change, and $w(t) = w_I(t) + jw_Q(t)$ is circularly symmetric complex AWGN with autocorrelation $\mathcal{R}_w(t) = \sigma_w^2\delta(t)$. The signal-to-noise-ratio (SNR) due to AWGN is a^2/σ_w^2 . Samples at times t_n , $n = 0, 1, \dots, N - 1$ are given as

$$r_n = a \exp\{j2\pi[ft_n + \theta + \eta_n]\} + w_n. \quad (5)$$

The principal argument of r_n is

$$\angle r_n = 2\pi[ft_n + \theta + \eta_n + \epsilon_n], \quad (\text{mod } 2\pi) \quad (6)$$

where ϵ_n describes the effective phase error due to the AWGN and is known as additive observation phase noise (AOPN) [14]. We further define the *unwrapped phase*

$$x_n = ft_n + \theta + \xi_n = y_n + u_n, \quad (7)$$

where $\xi_n = \eta_n + \epsilon_n$ is the total phase error, $y_n = \angle r_n/(2\pi)$ is the extracted *wrapped phase* (modulo 1), and $u_n \in \mathbb{Z}$ is the unknown integer number of cycles that must be added to the wrapped phase to perform phase unwrapping.

2.3. Phase Change Statistics

When the dominant source of laser phase noise is spontaneous emission, the frequency noise $\omega_n = d\phi_n/dt$ is assumed to be white and Gaussian [12]. Thus the frequency noise has a constant PSD $\mathcal{S}_{\omega_n}(\omega) = \Delta_\omega$, where $\Delta_\nu = \Delta_\omega/(2\pi)$ is the full-width at half-maximum laser linewidth in Hz, and is assumed to be known. Then the phase noise $\phi_n(t)$ is a Wiener process. For a fixed delay τ , the resulting phase change $\Delta\phi_n(t; \tau)$ in the interference signal is a zero-mean, stationary Gaussian process with triangular autocorrelation function

$$\mathcal{R}_{\Delta\phi_n}(t; \tau) = \Delta_\omega(\tau - |t|) \text{rect}\left(\frac{t}{2\tau}\right). \quad (8)$$

2.4. AOPN Statistics

Given $|r_n|$, the scaled AOPN term $2\pi\epsilon_n$ has a zero-mean von Mises distribution with a complicated dependence on a , $|r_n|$, and σ_w^2 [14]. Tretter observed that the AOPN distribution is approximately Gaussian with variance $1/(2 \cdot \text{SNR})$ at high SNR [5]. At low SNR, the von Mises distribution is approximately uniform over $(-\pi, \pi)$, so we propose an approximation to the AOPN variance that captures both SNR regimes:

$$\sigma_\epsilon^2 \approx \min\left\{\frac{\sigma_w^2}{(2\pi)^2 \frac{2}{N} \sum_{n=0}^{N-1} |r_n|^2}, \frac{1}{12}\right\}. \quad (9)$$

3. PROPOSED ALGORITHM

Our goal is to estimate frequency f from wrapped phase vector \mathbf{y} . However, directly maximizing the likelihood $p(\mathbf{y}|f, \theta)$ is difficult because the positions of the discontinuities in the wrapped phase \mathbf{y} are unknown. If one can recover the number of unwrappings \mathbf{u} , yielding the complete data $\mathbf{x} = \mathbf{y} + \mathbf{u}$, then maximizing $p(\mathbf{x}|f, \theta)$ is straightforward because \mathbf{x} is an affine function in correlated Gaussian noise.

Tretter introduced the approach of frequency estimation via phase unwrapping followed by linear regression [5]. Wang et al. further updated the frequency estimation procedure to account for both phase noise and AOPN [9]. However, these methods keep the unwrapping and regression steps separate, and since the naïve

Algorithm 1 Viterbi Unwrapping Frequency Estimation

Input: $\mathbf{y}, \{f_0^{(0)}, \dots, f_{M-1}^{(0)}\}, \{\theta_0^{(0)}, \dots, \theta_{M-1}^{(0)}\}$
Output: $\hat{f}, \hat{\theta}$

```

1: for  $m = 0, 1, \dots, M - 1$  do
2:    $L_m^{\text{best}} \leftarrow \infty, f_m^{\text{best}} \leftarrow f_m^{(0)}, \theta_m^{\text{best}} \leftarrow \theta_m^{(0)}$ 
3:    $k \leftarrow 0$ 
4:   while converged = false do
5:     compute  $\mathbf{Q}(f_m^{(k)})$ 
6:      $\hat{\mathbf{x}}_m^{(k)}, L^V(f_m^{(k)}, \theta_m^{(k)}) \leftarrow \text{UnwrapViterbi}(\mathbf{y}, f_m^{(k)}, \theta_m^{(k)})$ 
7:     if  $L^V(f_m^{(k)}, \theta_m^{(k)}) < L_m^{\text{best}}$  then
8:        $L_m^{\text{best}} \leftarrow L^V(f_m^{(k)}, \theta_m^{(k)})$ 
9:        $f_m^{\text{best}} \leftarrow f_m^{(k)}, \theta_m^{\text{best}} \leftarrow \theta_m^{(k)}$ 
10:       $f_m^{(k+1)}, \theta_m^{(k+1)} \leftarrow \text{GLS}(\hat{\mathbf{x}}_m^{(k)}, \mathbf{Q}(f_m^{(k)}))$ 
11:       $k \leftarrow k + 1$ 
12:     else
13:        $\hat{f}_m \leftarrow f_m^{\text{best}}, \hat{\theta}_m \leftarrow \theta_m^{\text{best}}$ 
14:       converged = true
15:  $\tilde{m} = \arg \min_m L_m^{\text{best}}$ 
16:  $\hat{f} \leftarrow \hat{f}_{\tilde{m}}, \hat{\theta} \leftarrow \hat{\theta}_{\tilde{m}}$ 

```

phase unwrapping algorithms (e.g., [15]) have no requirement for the underlying signal to be linear, unwrapping errors lead to further errors in the regression. More sophisticated algorithms jointly perform frequency estimation via phase unwrapping by alternating between two main steps: 1) estimating the missing data \mathbf{u} given a current estimate of the parameters $\hat{f}, \hat{\theta}$, and 2) updating the parameter estimates $\hat{f}, \hat{\theta}$ assuming the complete data $\mathbf{x} = \mathbf{y} + \mathbf{u}$ is known. For instance, the FLSPUE algorithm iterates between unwrapping the phase for a dense grid of candidate frequencies and then applying ordinary least squares (OLS) regression to refine and compute the best estimate [8]. However, the FLSPUE approach to unwrapping given a candidate frequency constrains the noise to be bounded within $[-1/2, 1/2)$, which is only a good approximation for uncorrelated noise with small variance. Our proposed algorithm likewise alternates between phase unwrapping and linear regression. However, we perform both steps more rigorously by accounting for the statistics of both correlated phase error and AOPN.

3.1. Viterbi Phase Unwrapping

We seek the maximum likelihood estimate of the sequence of integer-valued unwrappings \mathbf{u} , given the observed data \mathbf{y} and initial estimates of the frequency \hat{f} and phase offset $\hat{\theta}$. Assuming the sequence unwrapping is causal, and using a finite memory of length C , we can approximate the maximum likelihood estimate as

$$\begin{aligned} \hat{\mathbf{u}} &= \arg \max_{\mathbf{u}} p(\mathbf{y} | \mathbf{u}, \hat{f}, \hat{\theta}) \\ &\approx \arg \max_{\mathbf{u}} \prod_{n=0}^{N-1} p(y_n | u_n, \mathbf{y}_{n-C}^{n-1}, \hat{\mathbf{u}}_{n-C}^{n-1}, \hat{f}, \hat{\theta}), \end{aligned} \quad (10)$$

where $\mathbf{z}_k^\ell = [z_k, z_{k+1}, \dots, z_\ell]^T$ denotes the subset of a vector \mathbf{z} with indices $k \leq \ell$. The Viterbi algorithm estimates the maximum likelihood sequence by assigning a length (*branch metric*) to transitions between possible states (the unwrapping values u_n) and then recursively finding the sequence of states with the shortest path length. For each sample n , we use the previous C unwrapping estimates $\hat{\mathbf{u}}_{n-C}^{n-1}$ and the phase error correlation for causal LMMSE

prediction of the phase error at sample n :

$$\hat{\xi}_n^{\text{LMMSE}} = \mathbf{p}_C^T \mathbf{Q}_C^{-1} (\mathbf{y}_{n-C}^{n-1} + \hat{\mathbf{u}}_{n-C}^{n-1} - \hat{f} \mathbf{t}_{n-C}^{n-1} - \hat{\theta}), \quad (11)$$

where cross-covariance vector \mathbf{p}_C has elements

$$[\mathbf{p}_C]_k = \mathbb{E}[\eta_n \eta_{n-C+k}] + \mathbb{E}[\epsilon_n \epsilon_{n-C+k}], \quad (12)$$

auto-covariance matrix \mathbf{Q}_C has elements

$$[\mathbf{Q}_C]_{k\ell} = \mathbb{E}[\eta_{n-C+k} \eta_{n-C+\ell}] + \mathbb{E}[\epsilon_{n-C+k} \epsilon_{n-C+\ell}], \quad (13)$$

$k, \ell \in \{0, \dots, C-1\}$, and $\mathbf{t} = [t_0, t_1, \dots, t_{N-1}]^T$. Given the predicted phase error, the likelihood of each value of u_n is then

$$\begin{aligned} p(y_n | u_n, \mathbf{y}_{n-C}^{n-1}, \hat{\mathbf{u}}_{n-C}^{n-1}, \hat{f}, \hat{\theta}) \\ \approx \frac{1}{\sqrt{2\pi\sigma_e^2}} \exp \left\{ -\frac{(y_n + u_n - \hat{f}t_n - \hat{\theta} - \hat{\xi}_n^{\text{LMMSE}})^2}{2\sigma_e^2} \right\}, \end{aligned} \quad (14)$$

where $\sigma_e^2 = \sigma_\eta^2 + \sigma_\epsilon^2 - \mathbf{p}_C^T \mathbf{Q}_C^{-1} \mathbf{p}_C$ is the variance of the LMMSE estimator error. The branch metric is the negative log-likelihood

$$\lambda(u_n) = \frac{(y_n + u_n - \hat{f}t_n - \hat{\theta} - \hat{\xi}_n^{\text{LMMSE}})^2}{2\sigma_e^2} + \log(\sigma_e^2) \quad (15)$$

and a sequence of states has length $\sum_{n=0}^{N-1} \lambda(u_n)$. The most likely sequence has the shortest path, with length L^V . Note that unlike FLSPUE, our Viterbi unwrapping method encourages but does not constrain $\mathbf{y} + \hat{\mathbf{u}}$ to follow the hypothesized line $\hat{f}\mathbf{t} + \hat{\theta}$, allowing for correlated noise that may drift from the line. Since both f and $\mathcal{R}_{\Delta\phi_n}$ depend on τ in the FMCW lidar setting, \mathbf{Q}_C and \mathbf{p}_C can be computed given \hat{f} . The number of possible unwrappings at each time step is large, so we use per-survivor processing and only keep a fixed number of S survivor paths [16]. Viterbi unwrapping thus considers multiple possible unwrapping sequences and chooses the most likely one.

3.2. Generalized Least Squares Refinement

Based on the unwrapped phase estimate $\hat{\mathbf{x}} = \mathbf{y} + \hat{\mathbf{u}}$ computed from Viterbi phase unwrapping, we can refine \hat{f} and $\hat{\theta}$ by fitting an affine function. Defining $\mathbf{1}_N$ as a column vector of N ones, matrix $\mathbf{A} = [\mathbf{t}, \mathbf{1}_N]$, parameter vector $\mathbf{b} = [f, \theta]^T$, and \mathbf{Q}_N as the phase error auto-covariance for the entire length- N sequence, the GLS parameter estimates are

$$\hat{\mathbf{b}} = \arg \min_{\mathbf{b}} (\hat{\mathbf{x}} - \mathbf{A}\mathbf{b})^T \mathbf{Q}_N^{-1} (\hat{\mathbf{x}} - \mathbf{A}\mathbf{b}) \quad (16)$$

$$= (\mathbf{A}^T \mathbf{Q}_N^{-1} \mathbf{A})^{-1} \mathbf{A}^T \mathbf{Q}_N^{-1} \hat{\mathbf{x}}. \quad (17)$$

Because $\mathcal{R}_{\Delta\phi_n}(t; \tau)$ yields a banded Toeplitz matrix \mathbf{Q}_N , a circulant approximation to \mathbf{Q}_N enables inversion via the fast Fourier transform algorithm and is sufficiently accurate for N much larger than the band width [17].

3.3. Full Algorithm

Like the FLSPUE algorithm [8], we initialize our estimation procedure at a discrete set of M initial frequencies $\{f_0^{(0)}, \dots, f_{M-1}^{(0)}\}$ and phase offsets $\{\theta_0^{(0)}, \dots, \theta_{M-1}^{(0)}\}$. Starting with the an initial pair $f_m^{(0)}$ and $\theta_m^{(0)}$, we iteratively perform Viterbi phase unwrapping and refinement of \hat{f} and $\hat{\theta}$ as long as the L^V of the unwrapping sequence decreases. Then the final estimates of \hat{f} and $\hat{\theta}$ are the frequency/offset pair that produced the lowest L^V over all M grid points. Pseudocode is shown in Algorithm 1.

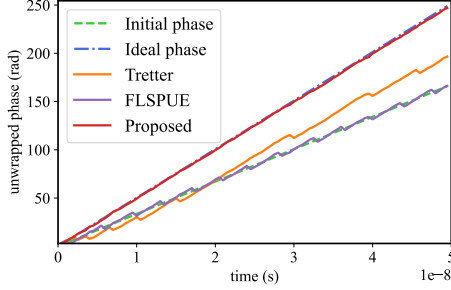


Fig. 3: Comparison of phase unwrapping methods for frequency estimation. Only our proposed Viterbi unwrapping method performs consistently well when phase error is significant.

4. NUMERICAL EXPERIMENTS

We first demonstrate in Fig. 3 the performance of our proposed Viterbi phase unwrapping algorithm compared to FLSPUE [8] and the naïve unwrapping used by Tretter [5]. The linewidth $\Delta\nu = 10$ MHz and the true distance is $d = 120$ m, resulting in highly-correlated, high-variance phase error. The naïve unwrapping performs poorly when the phase error variance is large, causing the frequency to be underestimated by Tretter’s method. Both FLSPUE and our Viterbi unwrapping are initialized with a frequency corresponding to 80 m, far from the true frequency. While FLSPUE unwrapping yields a bounded error distribution and thus has trouble deviating from the initial phase, our proposed approach converges to the true phase.

We next tested our proposed frequency estimation against existing algorithms, including periodogram maximization (Rife & Boorstyn [3]), naïve unwrapping and OLS regression (Tretter [5]), and Lorentzian fitting (Kim et al. [4]). We found FLSPUE did not achieve the best performance at any depth under any of the tested conditions, so the results are omitted. The simulation consists of 30 trials each at distances from 10 to 140 m in 10-m increments. Measurements consist of $N = 2 \times 10^4$ samples over measurement window $T_{\text{meas}} = 10 \mu\text{s}$. The source is swept over a bandwidth of 10 GHz (i.e., $\gamma = 1 \text{ GHz}/\mu\text{s}$) and has white frequency noise, with linewidths 1- and 10-MHz. For our proposed method, the Viterbi unwrapping algorithm uses a memory length $C = 1$, and the frequency estimation uses the Lorentzian estimate as the single initial frequency ($M = 1$).

Fig. 4 depicts the root mean square error (RMSE) performance versus distance for AWGN levels yielding SNRs of 20, 10, and 0 dB. We observe that periodogram maximization, often the default method for frequency estimation, is highly effective at low phase noise because there is a strong periodogram peak around the true depth. However, as the phase error increases with linewidth and/or distance, the signal PSD broadens, degrading the performance of peak-finding methods. Tretter’s method is even more sensitive to phase error, achieving the best performance overall only when the total phase error variance is small. Lorentzian fitting and our proposed method are far more consistent as a function of distance. Fig. 5 further shows that our proposed algorithm achieves a lower RMSE than Lorentzian fitting if the SNR is sufficiently high (i.e., above 7 dB) because the phase error prediction performance improves as the uncorrelated AOPN component diminishes. Otherwise, initializing our algorithm with the Lorentzian estimate yields similar performance at low SNR.

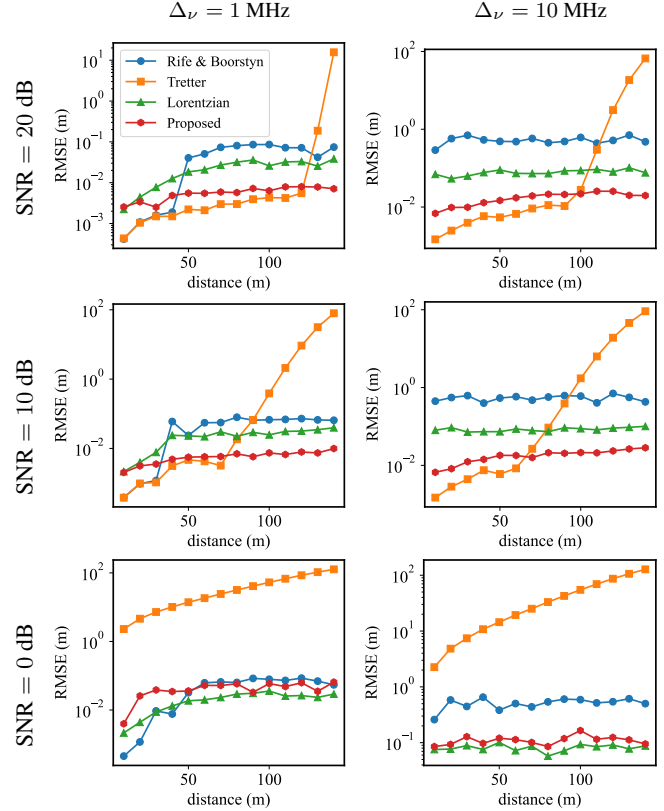


Fig. 4: Algorithm performance vs. distance for linewidths 1 and 10 MHz and SNR levels 20, 10, and 0 dB.

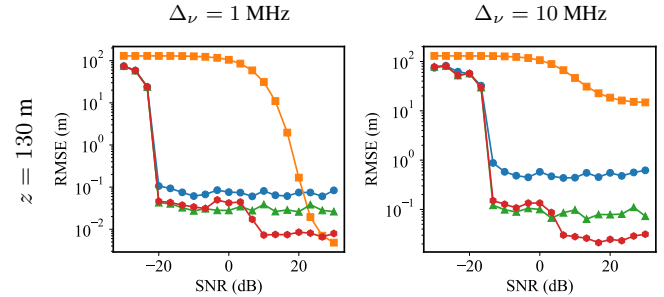


Fig. 5: Performance vs. SNR at $z = 130$ m. See legend in Fig. 4.

5. CONCLUSIONS

We have introduced an algorithm for accurate depth estimation from FMCW lidar measurements with significant phase noise and over long range. While Lorentzian fitting achieves good robustness overall, we show that phase unwrapping methods such as our algorithm can achieve even greater accuracy at high SNR. By handling large laser linewidths, our algorithm could enable the use of cheaper swept lasers with significant phase noise for use in FMCW lidar, SS-OCT, coherent communications, and other applications. Future work will aim to match the performance of Tretter’s method when the phase error variance is low.

6. REFERENCES

- [1] B. Behroozpour, P. A. Sandborn, M. C. Wu, and B. E. Boser, "Lidar system architectures and circuits," *IEEE Communications Magazine*, vol. 55, no. 10, pp. 135–142, Oct. 2017.
- [2] C. Henry, "Theory of the linewidth of semiconductor lasers," *IEEE Journal of Quantum Electronics*, vol. 18, no. 2, pp. 259–264, Feb. 1982.
- [3] D. Rife and R. Boorstyn, "Single tone parameter estimation from discrete-time observations," *IEEE Transactions on Information Theory*, vol. 20, no. 5, pp. 591–598, Sept. 1974.
- [4] T. Kim, P. Bhargava, and V. Stojanovic, "Optimal spectral estimation and system trade-off in long-distance frequency-modulated continuous-wave lidar," in *IEEE International Conference on Acoustics, Speech and Signal Processing (ICASSP)*, Apr. 2018, pp. 1583–1587.
- [5] S. Tretter, "Estimating the frequency of a noisy sinusoid by linear regression," *IEEE Transactions on Information Theory*, vol. 31, no. 6, pp. 832–835, Nov. 1985.
- [6] H. Fu and P. Y. Kam, "MAP/ML estimation of the frequency and phase of a single sinusoid in noise," *IEEE Trans. Sig. Proc.*, vol. 55, no. 3, pp. 834–845, Mar. 2007.
- [7] R. G. McKilliam, B. G. Quinn, I. V. L. Clarkson, and B. Moran, "Frequency estimation by phase unwrapping," *IEEE Transactions on Signal Processing*, vol. 58, pp. 2953–2963, June 2010.
- [8] Z. Xu, T. Lu, and B. Huang, "Fast frequency estimation algorithm by least squares phase unwrapping," *IEEE Signal Processing Letters*, vol. 23, no. 6, pp. 776–779, June 2016.
- [9] Q. Wang, Z. Quan, S. Bi, and P.-Y. Kam, "Joint ML/MAP estimation of the frequency and phase of a single sinusoid with Wiener carrier phase noise," *IEEE Trans. Sig. Proc.*, vol. 70, pp. 337–350, 2022.
- [10] A. Viterbi, "Error bounds for convolutional codes and an asymptotically optimum decoding algorithm," *IEEE Transactions on Information Theory*, vol. 13, no. 2, pp. 260–269, Apr. 1967.
- [11] A. Vasilyev, *The optoelectronic swept-frequency laser and its applications in ranging, three-dimensional imaging, and coherent beam combining of chirped-seed amplifiers*, Ph.D. dissertation, California Institute of Technology, 2013.
- [12] K. Petermann, *Laser diode modulation and noise*, Springer Netherlands, Dordrecht, 1988.
- [13] S. Banzhaf and C. Waldschmidt, "Phase-coded FMCW lidar," in *European Signal Processing Conference (EUSIPCO)*, Aug. 2021, pp. 1775–1779.
- [14] H. Fu and P.-Y. Kam, "Phase-based, time-domain estimation of the frequency and phase of a single sinusoid in AWGN—the role and applications of the additive observation phase noise model," *IEEE Transactions on Information Theory*, vol. 59, no. 5, pp. 3175–3188, May 2013.
- [15] R. W. Schafer, "Echo removal by discrete generalized linear filtering," Technical Report 466, MIT Research Laboratory of Electronics, Cambridge, MA, 1969.
- [16] R. Raheli, A. Polydoros, and C.-K. Tzou, "Per-Survivor Processing: a general approach to MLSE in uncertain environments," *IEEE Transactions on Communications*, vol. 43, no. 2/3/4, pp. 354–364, Feb. 1995.
- [17] R. M. Gray, "Toeplitz and circulant matrices: A review," *Foundations and Trends in Communications and Information Theory*, vol. 2, no. 3, pp. 155–239, Jan. 2006.